Desalination and Water Treatment
www.deswater.com

doi: 10.1080/19443994.2014.987826

57 (2016) 3654–3663
February

Taylor & Francis
Taylor & Francis Group

Application of raw, HCl- and H_2SO_4-activated bentonite as adsorbents for the removal of Zn^{2+} and Pb^{2+} from aqueous solution

Meghdad Rezapour[a,*], Hadi Abdollahi[b], Hamid Khorrami[a], Javad Taghavi Valmazuei[a]

[a]*Department of Mining and Metallurgical Engineering, Amirkabir University of Technology, Tehran 15875-4413, Iran, Tel. +98 93 60445312, Tel./Fax: +98 21 64542900; email: meghdad0111@yahoo.com (M. Rezapour), Tel. +98 93 53845200; email: h.khorrami@yahoo.com (H. Khorrami), Tel. +98 93 70715400; email: javad.taghavi.2008@gmail.com (J. Taghavi Valmazuei)*
[b]*School of Mining, College of Engineering, University of Tehran, Tehran 1439957131, Iran, Tel. +98 91 25032335; email: hadi_abdollahi2003@yahoo.com*

Received 17 February 2014; Accepted 4 November 2014

ABSTRACT

Raw and activated clay minerals were used as adsorbents for adsorbing Pb and Zn ions from an aqueous solution. Bentonite was activated using sulfuric and hydrochloric acids and sodium chloride. Activated bentonite with sulfuric and hydrochloric acids provided maximum adsorption of Pb and Zn ions as 490 mg L^{-1} (98%) and 275 mg L^{-1} (55%), respectively. The initial concentration of ions in solution was 500 mg L^{-1}. Minimum values of standard deviation for Pb and Zn ions were 0.06 and 0.03, and the values of coefficient of determination (R^2) for Pb and Zn ions were 0.996 and 0.998, respectively. Freundlich isotherm was preferred for describing the sorption of these metals. Furthermore, experimental results confirmed that the pseudo-first-order kinetic model was more suitable to interpret the mechanism of the sorption process.

Keywords: Raw; Activated bentonite; Na-bentonite; Adsorption; Aqueous solution

1. Introduction

Nowadays, scientists seek low-cost methods and materials for adsorption of organics and heavy metals. In recent decades, many researchers have studied adsorption system of heavy metal ions on natural and activated bentonite around the world [1–3]. For example, studying on the Algerian bentonite that was activated by HCl acid, the optimum parameters were indicated at $4 < pH < 6$, mass of adsorbent = 1 g, shaking time = 1 h, and initial concentration of metal ions was measured 10 mg L^{-1}. Results showed clay had significant potential for removing Zn^{2+}, Pb^{2+}, Cu^{2+}, and Ni^{2+} ions from polluted water [1]. Also, bentonite from Maghnia (NW, Algeria), the sorption of Co^{2+} ions indicated the pseudo-second-order kinetic model is the best fit and isotherm of Freundlich is more appropriate [2]. By Algerian bentonite clay, the removal efficiency of Pb^{2+} mostly was gotten to 92% while the initial concentration of metal ions and shaking time were 10 mg L^{-1} and 2 h, respectively. Conclusion of research determined significant potential for removing Pb^{2+} from wastewater using a low-cost adsorbent [3].

Na-bentonite was used for Pb(II) adsorption from aqueous solutions and the results showed that Pb(II)

---

*Corresponding author.

sorption is dependent on pH and ionic strength. In these experiments, the sorption percentage of Pb(II) was increased with increasing pH values at $pH < 7$, maintaining high level of sorption at pH 7–10 and at $pH > 10$, the heavy metal ions such as Pb^{2+} tend to form precipitation at high pH values, which limits the process greatly. This indicated that the sorption of Pb (II) on Na-bentonite can be explained by ion exchange or outer-sphere surface complexation at low pH values and by inner-sphere surface complexation at high pH values [4]. Also, adsorption results with the GMZ bentonite showed that the adsorption of Pb(II) on Na-bentonite depends on pH. Using thermodynamic data, it was shown that the adsorption of Pb(II) on Na-bentonite is an endothermic and spontaneous process [5]. Acid-activated montmorillonite was used as adsorbent for removal of 2,4,5-trichlorophenol (2,4,5-TCP) from aqueous solution, and the results indicated that by increasing adsorbent mass, pH, and temperature, the sorption of trichlorophenol per unit weight of the adsorbent decreased. However, an increase of adsorption was observed when initial concentration of trichlorophenol increased. Kinetic data fitted well with the pseudo-second-order rate expressions. Results indicated that the adsorption could be assigned to a physisorption model [6]. Adsorption of poly (1-vinylimidazole) on the Na-bentonite increased with increasing pH and decreasing ionic strength and temperature. It was shown that the high adsorption of poly (1-vinylimidazole) in the Na-bentonite was caused by electrostatic interactions at pH 8.5 [7]. Pb(II) was adsorbed by bentonite in raw, acid-activated, and manganese oxide-coated forms. The Langmuir monolayer adsorption capacities in 0.1 M KNO_3 solution were 16.70, 8.92, and 58.88 $mg\,g^{-1}$, respectively. Results showed the dependence of Pb(II) adsorption on the nature of the adsorbent surface [8]. Tomić et al. [9] treated bentonite from Petrovac and Aleksinac regions with sulfuric acid and studied their structure variation. Results demonstrated that the acid affected the octahedral sheets and therefore increased the specific surface area from 6 to 387 $m^2\,g^{-1}$ (bentonite from Petrovac) and from 11 to 306 $m^2\,g^{-1}$ (bentonite from Aleksinac) [9]. Also, Cu and Nickel ions were removed by Na-bentonite under static conditions. The adsorption equilibrium for nickel and copper was observed for 200 min. The adsorption capacities followed the order $Cu^{2+} > Ni^{2+}$ in single-component systems and the decreasing order of competitive adsorption capacities in binary component systems was $Cu^{2+} > Ni^{2+}$. The adsorption percentage followed the order $Cu^{2+} > Ni^{2+}$ at the same pH values [10]. Raw and acid-activated bentonites were used to adsorb blue methylene (BM) and zinc ions, and the results showed that the adsorption capacity of BM and Zn ions by raw bentonite were 2.2 and 1.1 $mmol\,g^{-1}$ of bentonite, respectively. The maximum uptake of BM and Zn ions weas reduced by acid-activated bentonite because of partial collapse of montmorillonite particles and formation of amorphous silica [11]. Adsorption and desorption of Cd(II) and Zn(II) on local bentonite were modeled. The maximum adsorptions for Zn and Cd were 99.85 and 96.84%, respectively, whereas the maximum desorption for Zn and Cd were found to be 6.57 and 51.37%, respectively. Also, the interactions of parameters such as the solid/liquid ratio, ultrasound power, and temperature, were an important factor in the various ratios for desorption of Cd(II) and Zn(II) [12]. Metal ions adsorption was studied for granular pillared that included organo- and inorgano-bentonites. Adsorption tests were performed with aqueous multi-metal solutions of Pb^{2+}, Cu^{2+}, Cd^{2+}, Zn^{2+}, and Ni^{2+} ions, with liquid dodecane and aqueous dodecane solutions. The smallest and highest adsorptions were observed for Al-pillared and granular organo-bentonite at 30 min and 12 h, respectively. Powdered inorgano–organo-bentonite had the maximum adsorption capacity at higher metal concentration and lower adsorbent content (Cu^{2+}: 2.2, Ni^{2+}: 1.7, Zn^{2+}: 1.4, Cd^{2+}: 0.9, and Pb^{2+}: 0.7 all in $mmol\,g^{-1}$) [13]. In this study, application of raw, HCl- and H_2SO_4-activated bentonite as adsorbents for the removal of Zn^{2+} and Pb^{2+} from aqueous solution were investigated. In this research, mechanism of adsorption such as Langmuir and Freundlich isotherms was considered and the effects of different influential parameters on the efficiency of the sorption process were studied.

2. Materials and methods

2.1. Characterization studies

Bentonite samples were obtained from the Rashm mine in the Semnan province of Iran. After obtaining a representative sample, optical microscopy, X-ray diffractometer (XRD), and XRF analysis were carried out and the results showed that the bentonite samples mainly consist of montmorillonite and minor amounts of quartz, calcite, crystobalite, gypsum, etc.

After crushing and preparation of the sample, high-grade adsorbent montmorillonite was obtained by sizing through a hydrocyclone.

XRD was used for determination of mineral types. XRD analysis was performed to indicate composition of adsorbents. Powder diffraction patterns were obtained with a Siemens D-500 diffractometer with Ni-filtered CuKα radiation and a goniometer speed of $1^\circ 2\theta\,min^{-1}$. XRF analysis (Siemens 303 SRS and

Philips magix pro) showed that Al_2O_3 and SiO_2 are major compounds in the sample and Na_2O, MgO, Fe_2O_3, CaO, and K_2O are minor oxides. These data are presented in Table 1.

2.2. Activating process of bentonite

After sizing and enrichment with hydrocyclone, the bentonite was activated by three kinds of activators, HCl, H_2SO_4, and NaCl. During activation process, various influential parameters such as temperature, contact time, and concentration of activators were considered. Activation process was performed with mechanical stirrer at 500 RPM (IKA overhead stirrer) at mild temperature as 348 K. During activation process, concentration of activators was 1 M. The optimized contact time was 8 h.

2.3. Batch adsorption experiments

2.3.1. Preparation of standard solutions

For making 1,000 mg L^{-1} of solutions with Pb and Zn ions, 1.6 g of $Pb(NO_3)_2$ and 4.4 g of $ZnSO_4$ $7H_2O$ were dissolved in 500 cc water. These concentrations were within the solubility range of metal salts. Concentration of ions in solutions including Pb^{2+} and Zn^{2+} ions for the experiments varied from 50 to 1,000 mg L^{-1}. In addition, a liquid/solid ratio of 20:1 (mL g^{-1}) was used in all experiments. Final concentrations of metal ions in the solution were measured in double readings with an atomic adsorption spectrometer (Varian AA 240Z, Germany).

2.3.2. Batch isotherm model

For simulation of adsorption process, Langmuir, Freundlich, and D–R equilibrium isotherms were used. Langmuir and Freundlich isotherms are presently being used to describe the adsorption characteristics of metal ions in water and wastewater treatment [14].

2.3.2.1. Langmuir isotherm. Langmuir adsorption isotherm was first used to describe the adsorption of gas molecules on metal surface [15–20]. This model has been used successfully to indicate many uptake models. Langmuir model is shown with the following Eq. (1):

$$q = \frac{K \times q_{\max} \times C_e}{1 + K \times C_e} \tag{1}$$

Eq. (1) is modified to a linear statement as Eq. (2):

$$\frac{C_e}{q_e} = \frac{1}{K \times q_{\max}} + \frac{C_e}{q_{\max}} \tag{2}$$

where q_e (mg g^{-1}) is the amount of metal ions adsorbed, q_m (mg g^{-1}) is the monolayer capacity of metal ions, C_e is the equilibrium concentration of metal ions, and K is the Langmuir constant (L mg^{-1}) related to free energy of adsorption.

The important factor for Langmuir isotherm is expressed as a constant separation factor. This parameter is a dimensionless equilibrium parameter, R_L, which can be calculated by the following equation [19]:

$$R_L = \frac{1}{(1 + K \times C_0)} \tag{3}$$

where K is the Langmuir constant and C_0 is the initial concentration of metal ion. R_L value indicates the approach to the isotherm. R_L values between 0 and 1 indicate favorable absorption. R_L values equal to zero

Table 1
XRF analysis of Rashm mine samples

Sample compound	RH (%)	RG (%)	RF (%)	RD(%)	RC (%)	RB(%)	RA (%)
Na_2O	6.80	6.60	7.90	7.70	8.40	8.50	8.20
MgO	2.57	2.46	3.05	3.59	1.66	1.79	1.92
Al_2O_3	11.50	11.30	13.40	12.00	9.20	9.20	9.30
SiO_2	62.10	62.30	60.00	61.60	65.80	65.10	66.70
K_2O	0.11	0.15	0.11	0.25	0.41	0.44	0.44
CaO	1.39	1.49	0.64	1.47	1.00	1.11	0.69
Fe_2O_3	1.75	1.74	2.01	1.68	0.64	0.67	0.66
L.O.I.	13.78	13.96	12.89	11.71	12.89	13.19	12.09
Total	100	100	100	100	100	100	100

indicate irreversible absorption, $R_L = 1$ shows linear adsorption, and $R_L > 1$ shows unfavorable adsorption [20,21].

2.3.2.2. Freundlich isotherm. Freundlich adsorption isotherm is applicable for adsorption on heterogeneous clay surfaces. Adsorption equilibrium data were applied to the Freundlich model in logarithmic form as follows [22,23]:

$$\log q_e = \log k_f + \frac{1}{n} \log C_e \tag{4}$$

where k_f and n are Freundlich constants related to adsorption capacity and adsorption intensity, respectively. In order to study the adsorption process, SD was calculated for each of the Langmuir and Freundlich isotherms to determine which is the more suitable model to describe the adsorption mechanism. The standard deviation (SD) was obtained as follows:

$$\mathrm{SD} = \sqrt{\frac{\sum[(qt_{\mathrm{exp}} - qt_{\mathrm{cal}})/qt_{\mathrm{exp}}]^2}{m-1}} \tag{5}$$

where qt_{exp} and qt_{cal} are adsorption parameters obtained from the experimental data and calculated from the sorption isotherm data, respectively. Also, m is the number of experiments performed in the laboratory. Results of the experimental data were normally close to data obtained from isotherms models. The best mechanism of the adsorption process is the one in which the SD of experimental data from the isotherms be close to zero [24].

2.3.3. Kinetic experiments

Adsorption kinetic tests were carried out for 10, 20, 30, 60, 120, and 180 min. with Pb and Zn concentrations of 300 mg L^{-1}. Kinetic studies were performed for raw, sulfuric acid-activated, HCl acid activated and Na-bentonites. Liquid/solid ratio was set to 20:1 (mL g^{-1}). The pH values in the adsorption process for Pb ions for raw and Na-bentonites varied between 4 and 5, but for the sulfuric acid and HCl-activated bentonites, the pH varied between 2.6 and 3. Also, the pH values in the adsorption process for Zn ions for raw and Na-bentonites varied between 6 and 7.4, but for the sulfuric acid and HCl-activated bentonites, it varied between 3.5 and 5. All the tests, were carried out at 294 K.

Adsorption kinetics is one of the most valuable properties being indicative for the efficiency of the adsorption phenomena. Kinetic models such as the pseudo-first-order equation proposed by Lagergren and the pseudo-second-order equation proposed by Ho have been utilized to predict adsorption kinetics from the experimental data.

2.3.3.1. The pseudo-first-order model. This model is expressed as follows:

$$\ln (q_1 - q_t) = \ln q_1 - k_1 t \tag{6}$$

where q_1 and q_t are the amount of metal ions adsorbed by adsorbent at the equilibrium times (mg g^{-1}) and k_1 is the rate constant of the Lagergren first-order model for adsorption process (min^{-1}). k_1 can be calculated from the slope of plots of ln $(q_1 - q_t)$ vs. t [24,25].

2.3.3.2. The pseudo-second-order kinetic model. Its equation is expressed as follows:

$$\frac{t}{q_t} = \frac{1}{k_2 \times q_2^2} + \left(\frac{1}{q_2}\right) t \tag{7}$$

where q_2 is the maximum adsorption capacity (mg g^{-1}) and k_2 is the constant rate of the pseudo-second-order model for adsorption process (g mg^{-1} min^{-1}). k_2 and q_2 values can be calculated from the plot of t/qt vs. t [24,26].

The adsorption model of inter-particle diffusion showed sorption of metal ions perching into the surface pore of adsorbent. The kinetic equation of this model can be written as follows [27]:

$$q_t = k_3 \times t^{\frac{1}{2}} + q_0 \tag{8}$$

where q_0 (mg g^{-1}) is the intercept and k_i is the inter-particle diffusion rate constant (mg g^{-1} min$^{-1/2}$). According to this model, if the plot of q_t vs. square root of time ($t^{1/2}$) is linear, inter-particle diffusion roles at the flow of adsorption and if these lines pass through the origin, inter-particle diffusion is the rate controlling step [28–31].

3. Results and discussion

3.1. Adsorption tests

After preparation and purification, the bentonite samples were heated in a furnace at 110˚C for 24 h and then dried. After drying, the samples were used in the adsorption tests. During the adsorption experiments, three influential parameters were considered *viz.* contact time, adsorbent, and initial metals concentration in solutions. In order to investigate the effect of initial metals concentration on the efficiency of adsorption process, solutions with initial metals concentrations of 50, 100, 200, 300, 500, and 1,000 mg L^{-1} were used. Tests were carried out with 100 mL of solution containing Pb or Zn ions with 5 g of adsorbent. Solution containing lead or zinc ions and adsorbent were mixed for 10 min at 500 rpm by mechanical mixer, but the total contact time was 3 h (mixing and settling time). Tests were repeated twice, and mean values were used for analysis. Next, the aqueous phase (including lead and zinc ions) was separated from solid (adsorbent) by a filter and analyzed by atomic adsorption spectrophotometer. Uptake percentage of metal ions (R%), and adsorbate amount per unit mass of adsorbent, q_0 (mg g^{-1}), was calculated using Eqs. (9) and (10) [32].

$$R = \frac{C_0 - C_e}{C_0} \times 100 \tag{9}$$

$$q = \left[\frac{C_0 - C_e}{M}\right] \times V \tag{10}$$

where R, q, C_0,C_e, V, and M are adsorbate percentage of metal ions (%), amount of adsorbate per unit mass of adsorbent (mg g^{-1}), initial metal concentrations (mg L^{-1}), equilibrium concentration of metal (mg L^{-1}), volume of solution (L), and dosage of adsorbent (mg), respectively.

Uptake percentage of lead and zinc metals before and after activation with sulfuric acid, hydrochloric acid, and salt (sodium chloride) is shown in Figs. 1 and 2 in which uptake percentages were increased after activation with different materials. Maximum adsorption of Pb and Zn at high concentration (500 mg L^{-1}) occurred after activation of bentonite with sulfuric and hydrochloric acids as 490 mg L^{-1} (98%) and 275 mg L^{-1} (55%), respectively.

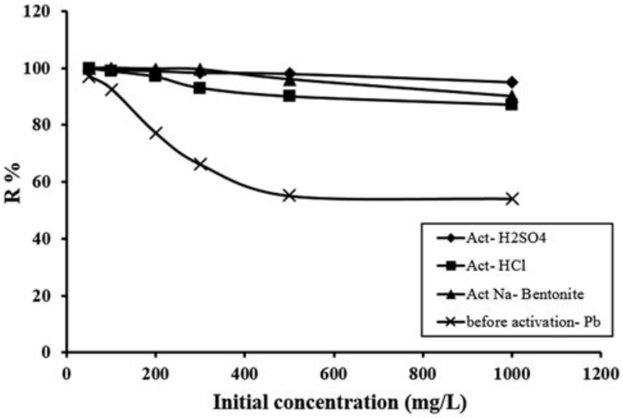

Fig. 1. Uptake percentage of lead in Montmorillonite samples before and after activation by sulfuric acid, hydrochloric acid and sodium chloride.

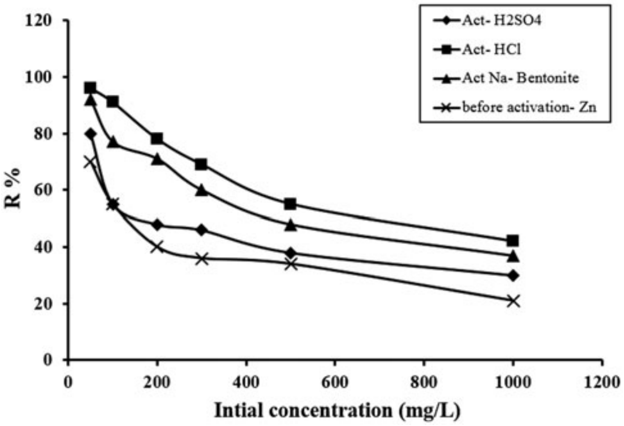

Fig. 2. Uptake percentage of zinc in Montmorillonite samples before and after activation by sulfuric acid, hydrochloric acid and sodium chloride.

3.2. Adsorption isotherms

3.2.1. Langmuir isotherm

Langmuir isotherm may be used more widely as the adsorption isotherm. Langmuir model is applied for individual cover layers on adsorption surface for which adsorption between molecules decreases [33]. For Langmuir model, C_e was plotted vs. C_e/q_e for lead and zinc ions for raw and adsorbents activated by sulfuric and hydrochloric acids and salt (sodium chloride) at initial metals concentrations of 50–1,000 mg L^{-1} (figures not shown). Parameters SD, R^2, k, and q_{max} were calculated for each case before and after activation which are presented in Table 2. The dimensionless constant R_L (called diffusion coefficient or equivalence parameter) was used for prediction of adsorption system of each lead and zinc ions. For both the ions, R_L values were between 0 and 1 which indicates that the tests are desirable (Tables 2 and 3).

3.2.2. Freundlich isotherm

Freundlich model is used to describe the adsorption process based on the assumption that adsorbent

Table 2
Langmuir and Freundlich isotherm constants for the adsorption of Pb^{2+} with the raw, HCl-activated, H_2SO_4-activated and Na-bentonite (Bentonite 5 g, Pb^{2+} concentrations: 50, 100, 200, 300, 500, 1,000 mg L^{-1}, $t = 3$ h.)

	Isotherm								
	Langmuir					Freundlich			
Samples	k	q_{max} (mg g^{-1})	R^2	SD	R_L (L mg^{-1})	k_f	n	R^2	SD
Raw	0.009	11.5	0.771	0.62	$0.1 < R_L < 0.69$	0.79	2.61	0.960	0.15
H_2SO_4-activated	0.139	21.27	0.944	0.42	$0.007 < R_L < 0.126$	2.91	2.07	0.996	0.06
HCl-activated	0.37	19.23	0.839	2.09	$0.002 < R_L < 0.051$	1.976	2.557	0.957	0.21
Na-bentonite	0.039	18.51	0.970	0.8	$0.025 < R_L < 0.34$	3.656	2.77	0.925	0.31

has a heterogeneous material made of different levels of adsorption positions. Adsorption on each of these levels follows the Langmuir model. Langmuir model does not show any adsorbate saturation on adsorbent but shows multilayer adsorption covered surface. Freundlich isotherms for lead and zinc ions are shown in Figs. 3 and 4. Data obtained from lead adsorption for all adsorbents are fitted on linear plot of ln q_e vs. ln C_e using the Freundlich equation. Related parameters are presented in Tables 2 and 3. K_f values for lead ions adsorbed by sodic adsorbent, raw, and adsorbents activated by HCl, H_2SO_4 are 3.656, 0.79, 1.976, and 2.91, respectively. Also, K_f values for zinc ions adsorbed by sodic adsorbent, raw, and adsorbents activated by HCl, H_2SO_4 are 0.482, 0.224, 0.762, and 0.212, respectively. Generally, the activation process increased the uptake capacities for lead and zinc ions. Normal SD for quantitative comparison of Langmuir and Freundlich isotherms is presented in Tables 2 and 3. Model data are comparable to experimental data and show that the values of SD are small. Small values for the model showed that it is able to describe adsorption of adsorbate on the adsorbent. According to the results presented in Tables 2 and 3, SD for lead ion are between 0.771 and 0.97 and for zinc ion between 0.24 and 0.58 in the Langmuir isotherm. In the Freundlich isotherm, SD for lead ion are between 0.06 and 0.31 and for zinc ion between 0.03 and 0.25, respectively.

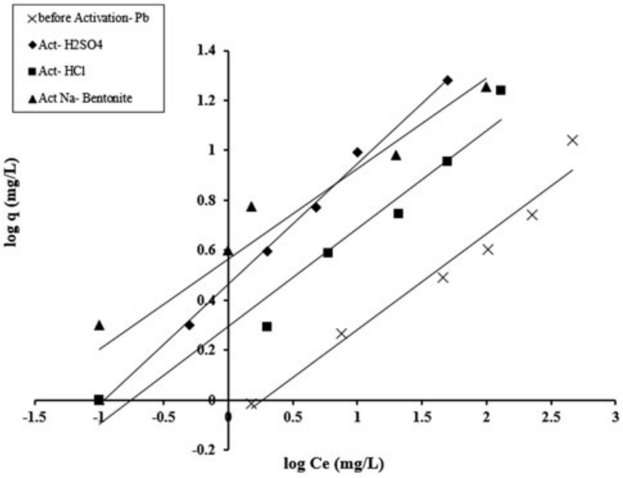

Fig. 3. Linear plot of Freundlich isotherm for the adsorption of Pb^{2+} with the raw, HCl-, H_2SO_4-activated and Na-bentonite. (Bentonite 5 g, Pb^{2+} concentrations: 50, 100, 200, 300, 500, 1,000 mg L^{-1}, $t = 3$ h.)

Table 3
Langmuir and Freundlich isotherm constants for the adsorption of Zn^{2+} with the raw, HCl-activated, H_2SO_4-activated and Na-bentonite (Bentonite 5 g, Zn^{2+} concentrations: 50, 100, 200, 300, 500, 1,000 mg L^{-1}, $t = 3$ h.)

	Isotherm								
	Langmuir					Freundlich			
Samples	k	q_{max} (mg g^{-1})	R^2	SD	R_L (L mg^{-1})	k_f	n	R^2	SD
Raw	0.007	4.81	0.963	0.24	$0.125 < R_L < 0.74$	0.224	2.197	0.912	0.18
H_2SO_4-activated	0.004	7.7	0.893	0.3	$0.2 < R_L < 0.83$	0.212	2.016	0.96	0.16
HCl-activated	0.0144	8.93	0.954	0.41	$0.065 < R_L < 0.58$	0.764	2.681	0.998	0.03
Na-bentonite	0.009	8.2	0.948	0.58	$0.1 < R_L < 0.69$	0.482	2.392	0.988	0.25

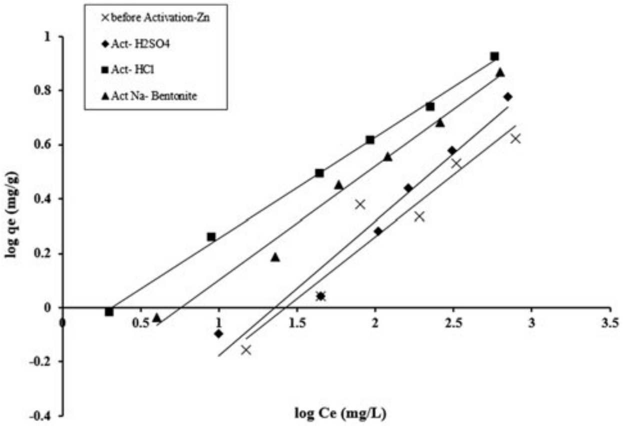

Fig. 4. Linear plot of Freundlich isotherm for the adsorption of Zn^{2+} with the raw, HCl-, H_2SO_4-activated and Na-bentonite. (Bentonite 5 g, Zn^{2+} concentrations: 50, 100, 200, 300, 500, 1,000 mg L^{-1}, $t = 3$ h.)

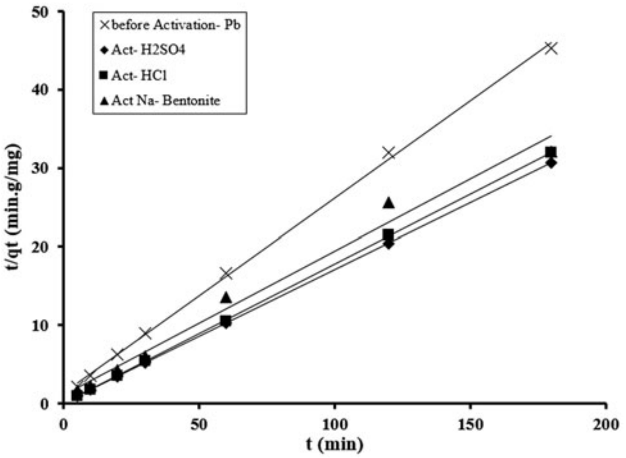

Fig. 5. Fit pseudo-second-order of adsorption of Pb^{2+} with the raw, HCl-, H_2SO_4-activated and Na-bentonite. (Bentonite 5 g, contact time: 5, 10, 20, 30, 60, 120, 180 min, $T = 294$ K.)

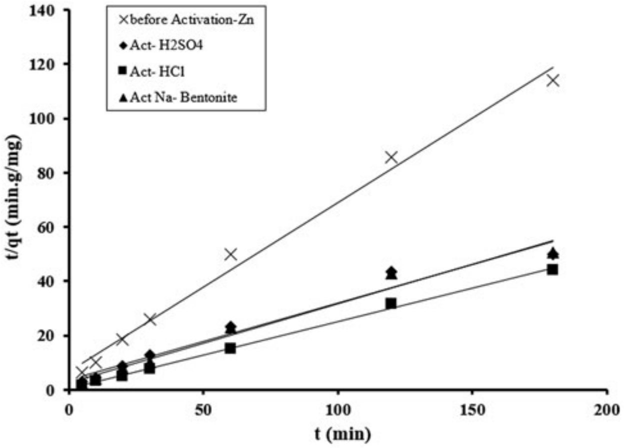

Fig. 6. Fit pseudo-second-order of adsorption of Zn^{2+} with the raw, HCl-, H_2SO_4-activated and Na-Bentonite. (Bentonite 5 g, contact time: 5, 10, 20, 30, 60, 120, 180 min, $T = 294$ K.)

3.3. *Kinetic of adsorption process*

In these series of tests, 100 mL of solutions with initial concentration of 300 mg L^{-1} was used at times of 5, 10, 20, 30, 60, 120, and 180 min. Initial pH varied between 2.6 and 5 for lead containing solutions and between 3.5 and 7.4 for zinc ions. Amount of adsorbent in solution was 5 g. Adsorption kinetic data were fitted to the pseudo-first-order model based on the Eq. (6) and to the pseudo-second-order model based on the Eq. (7). Diffusion adsorption (inter-particle) was considered according to the Eq. (8) [34]. Best conformity of data for both ions was related to second-order equation in which t/q_t is plotted vs. t (Figs. 5 and 6). All calculated parameters, q_1 and k_1 for first-order equation, q_2 and K_2 for second-order equation, and q_0 and k_0 for inter-particle effects, are presented in Tables 4 and 5. These figures show good fit of kinetic model with adsorption of Pb^{2+} and Zn^{2+} on the raw, HCl-activated, H_2SO_4-activated, and Na-bentonite adsorbents as explained by the pseudo-second-order equation (Eq. (7)). Values of the K_2 and q_2 for Pb^{2+} varied between 0.031 and 1.42 g mg^{-1} min^{-1} and 4.04 and 5.92 mg g^{-1}, respectively (Table 4) and for Zn^{2+} varied between 0.022 and 0.123 g mg^{-1} min^{-1} and 1.6 and 4.05 mg g^{-1}, respectively (Table 5). These parameters were calculated from the intercept and slope of Eq. (7). The correlation coefficient of the pseudo-second-order equation for the linear plot is 98.4–100, which suggests that the kinetics of adsorption can be described by the pseudo-second-order equation. For four kinds of adsorbent and for two metal ions (Pb^{2+} and Zn^{2+}), q_t was plotted vs. $t^{0.5}$ (Figs. 7 and 8) and their parameters were calculated which are presented in Tables 4 and 5. If the plot of q_t vs. $t^{0.5}$ is a straight line, then the adsorption process is just controlled by internal diffusion and the slope gives the rate constant K_i. However, if the data exhibit multi-linear plots, then two or more steps influence the sorption process [34]. According to Figs. 7 and 8, these plots do not fit a straight line, i.e. two or more processes interfere with adsorption mechanism. In addition to internal diffusion, other mechanisms influence the rate of adsorbate adsorption on adsorbent.

Table 4
Parameters of pseudo-first-order, pseudo-second-order and internal bit diffusion kinetics for adsorption of Pb^{2+}

	Pseudo-first-order			Pseudo-second-order			Internal bit diffusion		
Kinetic model sample	q_1 (mg g^{-1})	K_1 (min^{-1})	R^2	q_2 (mg g^{-1})	K_2 (g mg^{-1} min^{-1})	R^2	q_0 (mg g^{-1})	K_i (mg g^{-1} $min^{-1/2}$)	R^2
Raw	3.11	0.002	0.788	4.04	0.046	0.998	2.477	0.122	0.856
H_2SO_4-activated	0.3	0.006	0.466	5.92	0.4	1	5.502	0.035	0.393
HCl-activated	0.46	0.002	0.091	5.65	1.42	0.999	5.363	0.027	0.205
Na-bentonite	1.97	0.007	0.619	5.46	0.031	0.984	3.362	0.135	0.499

Table 5
Parameters of pseudo-first-order, pseudo-second-order and internal bit diffusion kinetics for adsorption of Zn^{2+}

	Pseudo-first-order			Pseudo-second-order			Internal bit diffusion		
Kinetic model sample	q_1 (mg g^{-1})	K_1 (min^{-1})	R^2	q_2 (mg g^{-1})	K_2 (g mg^{-1} min^{-1})	R^2	q_0 (mg g^{-1})	K_i (mg g^{-1} $min^{-1/2}$)	R^2
Raw	4.05	0.001	0.91	1.6	0.06	0.99	0.757	0.061	0.954
H_2SO_4-activated	3.07	0.003	0.906	3.53	0.022	0.966	1.604	0.132	0.9
HCl-activated	1.48	0.002	0.36	4.05	0.123	0.998	3.207	0.071	0.47
Na-bentonite	2.66	0.002	0.711	3.43	0.035	0.972	2.088	0.093	0.701

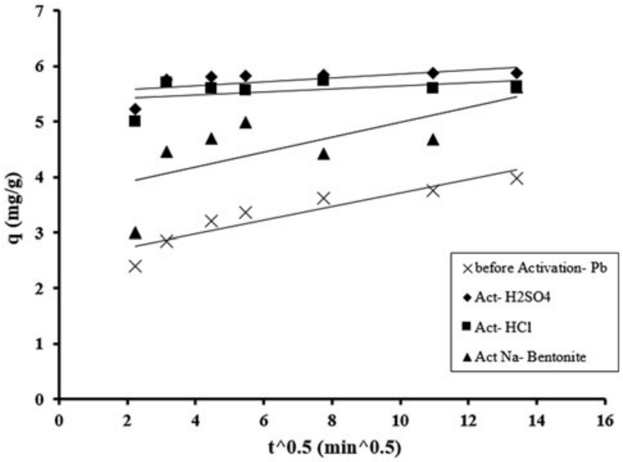

Fig. 7. Plots of internal bit diffusion kinetics of Pb^{2+} with the raw, HCl-, H_2SO_4-activated and Na-bentonite. (Bentonite 5 g, contact time: 5, 10, 20, 30, 60, 120, 180 min, $T = 294$ K.)

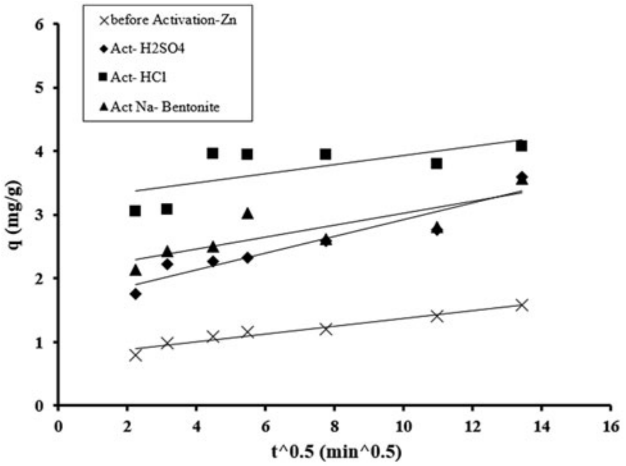

Fig. 8. Plots of Internal bit diffusion kinetics of Zn^{2+} with the raw, HCl-, H_2SO_4-activated and Na-bentonite. (Bentonite 5 g, contact time: 5, 10, 20, 30, 60, 120, 180 min, $T = 294$ K.)

4. Conclusion

Bentonite samples were obtained from Rashm mine–north of Iran. Optical microscopy, XRD, and XRF analysis showed that bentonites mainly consist of montmorillonite and minor amounts of quartz, calcite, crystobalite, and gypsum. Al_2O_3 and SiO_2 are major compounds in the sample, and Na_2O, MgO, Fe_2O_3, CaO, and K_2O are the minor oxides. After purification and activation with acids and sodium chloride, adsorption experiments were carried out. Results of isotherms studies showed that the Freundlich isotherm has a better conformity for adsorption of both contaminants. In the case of sulfuric acid-activated adsorbent for lead ion, minimum SD and maximum correlation factor (R^2)

were 0.06 and 0.996, respectively. In contrast, the minimum SD and maximum correlation factor (R^2) for zinc ion were 0.03 and 0.998 in the case of hydrochloric acid- activated adsorbent. Experimental data based on the kinetic models of pseudo-first-order model and pseudo-second-order model showed that these models were more suitable for describing the mechanism of these types of adsorbents. For the lead ion, the correlation factor was 100% for sulfuric acid-activated adsorbent, and for zinc, this value was 99.8% for the hydrochloric acid-activated adsorbent. Inter-particle diffusion studies for both lead and zinc ions for these types of adsorbents showed that the experimental data are not linear, so it cannot be completely influenced by diffusion effect, and there are other factors which affect the adsorption mechanism. Furthermore, the results showed that the highest efficiency of adsorption process for lead ion was obtained with adsorbent activated by sulfuric acid, but for adsorption of zinc ion, hydrochloric acid- activated adsorbent is preferred.

Acknowledgement

We are grateful to Dr Abbas Fazeli (Head of Mineral Processing Division in the Geological Survey of Iran) for scientific assistance. We also wish to thank our honorable partners on the project for their contributions to the work reported in this study.

References

[1] F. Mohammed-Azizi, S. Dib, M. Boufatit, Removal of heavy metals from aqueous solutions by Algerian bentonite, Desalin. Water Treat. 51 (22–24) (2013) 4447–4458.

[2] H. Assameur, M. Boufatit, Contribution to the removal study of Co^{2+} ions by acid-activated clay from Maghnia (Algeria): Equilibrium and kinetic studies, Desalin. Water Treat. 45 (1–3) (2012) 315–323.

[3] S. Dib, M. Boufatit, Equilibrium study of adsorption of Pb^{2+} from aqueous solution onto Algerian bentonite clay, Desalin. Water Treat. 5 (2009) 106–110.

[4] S. Yang, D. Zhao, H. Zhang, S. Lu, L. Chen, X. Yu, Impact of environmental conditions on the sorption behavior of Pb(II) in Na-bentonite suspensions, J. Hazard. Mater. 183 (2010) 632–640.

[5] S. Wang, Y. Dong, M. He, L. Chen, X. Yu, Characterization of GMZ bentonite and its application in the adsorption of Pb(II) from aqueous solutions, Appl. Clay. Sci. 43 (2009) 164–171.

[6] H. Zaghouane Boudiaf, M. Boutahala, Kinetic analysis of 2,4,5-trichlorophenol adsorption onto acid-activated montmorillonite from aqueous solution, Int. J. Miner. Process. 100 (2011) 72–78.

[7] N. Tekin, Y. Ateş, Adsorption of poly(vinylimidazole) from aqueous solutions onto Na-bentonite, Int. J. Miner. Process. 112–113 (2012) 49–54.

[8] E. Eren, B. Afsin, Y. Onal, Removal of lead ions by acid activated and manganese oxide-coated bentonite, J. Hazard. Mater. 161 (2009) 677–685.

[9] Z.P. Tomić, V.P. Logar, B.M. Babic, J.R. Rogan, P. Makreski, Comparison of structural, textural and thermal characteristics of pure and acid treated bentonites from Aleksinac and Petrovac (Serbia), Spectrochim. Acta. A. Mol. Biomol. Spectrosc. 82 (2011) 389–395.

[10] Z.R. Liu, S.-q. Zhou, Adsorption of copper and nickel on Na-bentonite, Process. Safe. Environ. Protec. 88 (2010) 62–66.

[11] M. Hajjaji, H. El Arfaoui, Adsorption of methylene blue and zinc ions on raw and acid-activated bentonite from Morocco, Appl. Clay Sci. 46 (2009) 418–421.

[12] O. Lacin, B. Bayrak, O. Korkut, E. Sayan, Modeling of adsorption and ultrasonic desorption of cadmium(II) and zinc(II) on local bentonite, J. Colloid Interface Sci. 292 (2005) 330–335.

[13] C.O. Ouellet-Plamondon, R.J. Lynch, A.A. Al-Tabbaa, Comparison between granular pillared, organo- and inorgano–organo-bentonites for hydrocarbon and metal ion adsorption, Appl. Clay. Sci. 67–68 (2012) 91–98.

[14] L. Metcalf, H.P. Eddy, G. Tchobanoglous, Wastewater engineering: Treatment, disposal, and reuse, in: McGraw-Hill Series in Water Resources and Environmental Engineering, New York, NY, 2004.

[15] I. Langmuir, The adsorption of gases on plane surfaces of glass, mica and platinum, J. Am. Chem. Soc. 40 (1918) 1361–1403.

[16] D. Xu, X.L. Tan, C.L. Chen, X.K. Wang, Adsorption of Pb(II) from aqueous solution to MX-80 bentonite: Effect of pH, ionic strength, foreign ions and temperature, Appl. Clay Sci. 41 (2008) 37–46.

[17] S. Chegrouche, A. Mellah, S. Telmoune, Removal of lanthanum from aqueous solutions by natural bentonite, Water Res. 31 (1997) 1733–1737.

[18] X. Wang, W. Dong, Z. Tao, A multitracer study on the adsorption of 32 elements on a natural hematite (α-Fe_2O_3): Effects of pH and fulvic acid, Colloids Surf. A 223 (2003) 135–143.

[19] N. Ahalya, R.D. Kanamadi, T.V. Ramachandra, Biosorption of chromium (VI) from aqueous solutions by the husk of Bengal gram (*Cicer arientinum*), Elec. J. Biotechnol. 8 (2005) 258–264.

[20] G. McKay, H.S. Blair, J.R. Gardner, Adsorption of dyes on chitin, I. Equilibrium studies, J. Appl. Polym. Sci. 27 (1982) 3043–3057.

[21] J.C. Igwe, A.A. Abia, Adsorption isotherm studies of Cd (II), Pb (II) and Zn (II) ions bioremediation from aqueous solution using unmodified and EDTA-modified maize cob, Eclética Química 32 (2007) 33–42.

[22] H. Freundlich, Ueber Die Adsorption in Loesungen (About the adsorption in the solutions), Engelmann, Leipzig, 1906.

[23] K.Y. Foo, B.H. Hameed, Insights into the modeling of adsorption isotherm systems, Chem. Eng. J. 156 (2010) 2–10.

[24] S. Lagergren, Zur theorie der sogenannten adsorption geloster stoffe. Kungliga Svenska Vetenskapsakademiens (The theory of the adsorption of the dissolved substances), J. Hand. 24 (1898) 1–39.

[25] A. Safa Özcan, Ö. GÖk, A. Özcan, Adsorption of lead (II) ions onto 8-hydroxy quinoline-immobilized bentonite, J. Hazard. Mater. 161 (2009) 499–509.

[26] Y.S. Ho, G. Mckay, Kinetic models for the sorption of dye from aqueous solution by wood, Process Saf. Environ. Protec. 76 (1998) 183–191.

[27] W.J. Weber, J.C. Morris, Kinetics of adsorption on carbon from solution, J. Sanit. Eng. Div. Am. Soc. Civ. Eng. 89 (1963) 53–55.

[28] A. Safa Özcan, Ş. Tetik, A. Özcan, Adsorption of acid dyes from aqueous solutions onto sepiolite, Sep. Sci. Technol. 39 (2005) 301–320.

[29] K.G. Bhattacharyya, A. Sharma, *Azadirachta indica* leaf powder as an effective biosorbent for dyes: A case study with aqueous Congo Red solutions, J. Environ. Manage. 71 (2004) 217–229.

[30] V.C. Srivastava, I.D. Mall, I.M. Mishra, Equilibrium modelling of single and binary adsorption of cadmium and nickel onto bagasse fly ash, Chem. Eng. J. 117 (2006) 79–91.

[31] J. Coggan, D. Stead, J. Howe, Application of surveying techniques for monitoring and appraisal of excavated China clay slopes, in: Adam Chrzanowski (Ed.), Proceedings of the 10th FIG International Symposium on Deformation Measurements, Orange, CA, 2001, pp. 240–249.

[32] D. Doulia, C.H. Leodopoulos, K. Gimouhopoulos, F. Rigas, Adsorption of humic acid on acid-activated Greek bentonite, J. Coll. Interface Sci. 340 (2009) 131–141.

[33] N. Jović-Jovičić, A. Milutinović Nikolić, P. Banković, Z. Mojović, M. Žunić, I. Gržetić, D. Jovanović, Organo–inorganic bentonite for simultaneous adsorption of acid orange 10 and lead ions, Appl. Clay. Sci. 47 (2010) 452–456.

[34] O.A. Ekpete, M. Horsfall Jr., A.I. Spiff, P. Adowei, Kinetics of phenol adsorption onto commercial and fluted pumpkin activated carbon in aqueous systems during batch analysis, Innov. Sci. Eng. 2 (2012) 62–71.